Ultrafiltration separation of nanoscale Am(VI)-polyoxometalate clusters from lanthanides

Thomas Albrecht-Schoenzart (talbrechtschoenzart@gmail.com)
Florida State University https://orcid.org/0000-0002-2989-3311
Hailong Zhang
Soochow University
Ao Li
Soochow University
Kai Li
Soochow University
Zhipeng Wang
Tsinghua University
Xiaocheng Xu
Tsinghua University
Yaxing Wang
Soochow University https://orcid.org/0000-0002-1842-339X
Matthew V. Sheridan
Soochow University
Hanshi Hu
Tsinghua University
Chao Xu
Tsinghua University
Evgeny Alekseev
Institute of Energy and Climate Research
Zhifang Chai
Soochow University
Shuao Wang
State Key Laboratory of Radiation Medicine and Protection, Soochow University
https://orcid.org/0000-0002-1526-1102

Physical Sciences - Article

Keywords:

Posted Date: April 1st, 2022

DOI: https://doi.org/10.21203/rs.3.rs-1454543/v1

Ultrafiltration separation of nanoscale Am(VI)-polyoxometalate clusters from lanthanides

Hailong Zhang[1]†, Ao Li[1]†, Kai Li[1]†, Zhipeng Wang[2], Xiaocheng Xu[3], Yaxing Wang[1]*, Matthew V. Sheridan[1], Han-Shi Hu[3], Chao Xu[2]*, Evgeny V. Alekseev[5], Zhifang Chai[1], Thomas E. Albrecht-Schönzart[4]*, Shuao Wang[1]*

[1]*State Key Laboratory of Radiation Medicine and Protection, School for Radiological and interdisciplinary Sciences (RAD-X) and Collaborative Innovation Center of Radiation Medicine of Jiangsu Higher Education Institutions, Soochow University, Suzhou 215123, China*

[2]*Institute of Nuclear and New Energy Technology, Tsinghua University, Beijing 100084, China*

[3]*Department of Chemistry and Laboratory of Organic Optoelectronics & Molecular Engineering of the Ministry of Education, Tsinghua University, Beijing 100084, China*

[4]*Department of Chemistry and Biochemistry, Florida State University, Tallahassee, Florida 32306, United States*

[5]*Institute of Energy and Climate Research, Forschungszentrum Jülich GmbH, D-52428 Jülich, Germany*

†*These authors contributed equally to this work.*

Email: yxwang@suda.edu.cn (Y. W.); xuchao@tsinghua.edu.cn (C. X.); tschoenzart@mines.edu (T. E. A.-S.); shuaowang@suda.edu.cn (S. W.).

Abstract: Partitioning of americium from lanthanides (Ln) present in used nuclear fuel plays a key role in the sustainable development of nuclear energy. This task is challenging because of the chemical similarities between Am(III) and Ln(III). Oxidization of Am(III) to Am(VI) has the potential to facilitate separations in principle, but rapid reduction of Am(VI) back to Am(III) by radiolysis products and organic reagents required for the traditional solvent extraction/solid extraction processes hampers practical redox-based separations. Herein, we report a nanoscale polyoxometalate (POM) cluster with a vacancy site compatible with the selective coordination of hexavalent actinides (^{238}U, ^{237}Np, ^{242}Pu, and ^{243}Am) over trivalent lanthanides in nitric acid media. This cluster is the most stable Am(VI) species in aqueous media observed to date. Ultrafiltration-based separation of nanoscale Am(VI)-POM clusters from hydrated lanthanide ions by commercially-available, fine-pored membranes enables the development of a once-through americium/lanthanide separation strategy that is highly efficient, rapid, environmentally benign, and requires minimal energy input.

Main

Americium is a neutron-capture byproduct of nuclear power generation and a major contributor to the long-term radiotoxicity of high-level waste (HLW)[1]. The efficient recovery of americium followed by transmutation into short-lived or stable nuclides using fast reactors would significantly reduce the environmental impact of nuclear energy[2]. However, the coexistence of lanthanides (Ln) with high neutron capture cross sections (*e.g.* ^{157}Gd) severely limits transmutation efficiency. Overcoming this impediment requires the development of efficient separations between americium and lanthanides and has remained a long-standing challenge in the nuclear industry for decades[3]. This difficulty originates primarily from their similar chemical behavior because both americium and lanthanides exist in solution as thermodynamically stable trivalent cations that possess nearly identical ionic radii and coordination chemistry. Traditional separations exploits the subtle bonding differences between Am(III) and Ln(III) ions where nitrogen- or sulfur donor-containing extractants enable preferential partitioning of Am(III) over Ln(III)[4, 5]. This separation strategy, however, is still hampered by limited discrimination between Am(III) and Ln(III), and, more importantly, by the generation of large amounts of secondary radioactive liquid waste.

One proposed method for mitigating this separation challenge is the oxidation of Am(III) to the higher oxidation states of Am(V) and Am(VI). These cations possess coordination chemistry that parallels the linear dioxo early actinyl ions such as UO_2^{2+} and NpO_2^{+} with anisotropic coordination that contrasting sharply with relatively isotropic Ln(III) ions[6]. This, in principle, leads to better discrimination between americium and lanthanides and a subsequent increase in separation efficiency. Although various techniques have been explored following this route, including solvent extraction[7, 8], precipitation[9], and ion-exchange chromatography[10], an unsolved issue is unavoidable reduction of high-valent Am back to Am(III) during the separation process. Am(VI) cations are strong oxidizing agents with reduction potentials of 1.6 V and 1.68 V for AmO_2^{2+}/AmO_2^{+} and AmO_2^{2+}/Am^{3+} couples, respectively (*versus* SHE)[11]. Therefore, Am(III) species can be produced in a few seconds once Am(VI) ions contact organic extractants/solvents or pass through a chromatographic column, making these separations impractical. In fact, both Am(VI) and Am(V) are traditionally thought to be unstable in aqueous solution because they can even be efficiently reduced by radiolysis products given that the two common americium isotopes related to the nuclear fuel cycle (^{241}Am and ^{243}Am) are both considerably radioactive.

In this work, we address these challenges by selecting a polyoxometalate (POM) that is tailored for the coordination requirements of Am(VI) and discriminates against Ln(III) cations. POMs are a well-known class of nanoscale, inorganic, metal-oxo clusters assembled from MO_x units (M = V, Mo, W, x = 4-6)[12]. This POM is equipped with a vacant equatorial donor site precisely matching the common pentagonal bipyramid coordination geometry of an actinyl ion and is unsuitable for binding Ln(III) ions. Such precise and strong coordination by a large cluster not only stabilizes Am(VI) to an unmatched level but also efficiently discriminates americium and lanthanides with a large size difference between their coexisting chemical species (Fig. 1). When

combined with an industrial ultrafiltration technique, these efforts give rise to a new separation method.

The lacunary POM {Se_6W_{46}} was synthesized through self-assembly of the {Se_6W_{39}} precursor[13, 14] in acid solution at room temperature (detailed synthetic procedures can be found in the supplementary information). The initial {Se_6W_{39}} possesses a macrocyclic structure with a cavity size of 8.7 × 8.7 Å. After self-assembly, one cap of the cavity is plugged by four WO_6^{6-} groups, and the other side is capped by three WO_6^{6-} groups, leaving a vacancy site with pre-organized coplanar oxo-donor structure for binding actinyl ions (Fig. 1 and Fig. S1), as demonstrated by single X-ray diffraction analysis. We observed that {Se_6W_{46}} is prone to form nanoscale clusters in nitric acid. As shown in Fig. S2, dynamic light scattering measurements indicate that the hydrodynamic diameter of {Se_6W_{46}} is ca. 2.6 nm, consistent with the crystallographic result in the dimension of 2.02 × 2.02 × 1.02 nm. Raman spectra recorded from solutions of {Se_6W_{46}} stored in 0.1 M nitric acid for one week revealed that it has the sufficient stability to be used in these harsh conditions (Fig. S3).

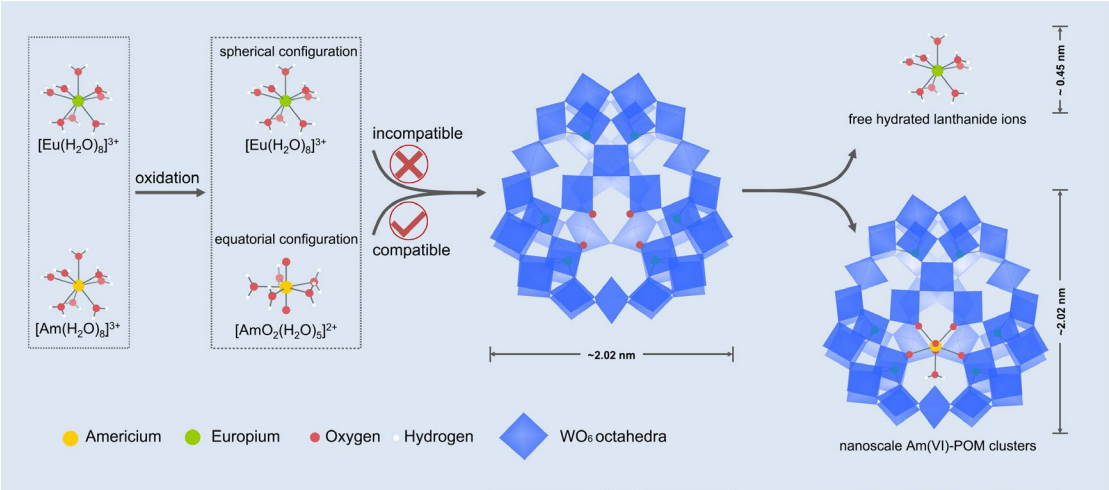

Fig. 1 Graphical representation of the ultrafiltration separation of nanoscale Am(VI)-polyoxometalate clusters from lanthanides.

To investigate the complexation properties of actinyl ions with the POM cluster in nitric acid, we monitored the change in the absorption spectra of AnO_2^{2+} ions (An = ^{238}U, ^{237}Np, ^{242}Pu, or ^{243}Am) with the addition of the {Se_6W_{46}} POM. The absorption of UO_2^{2+}-{Se_6W_{46}} displays the typical charge transfer of the uranyl cation as shown in Figure 2a. The characteristic absorption bands of NpO_2^{2+}, PuO_2^{2+}, AmO_2^{2+} experience notable bathochromic shifts upon POM addition (Np(VI) from 1224 to 1251 nm, Pu(VI) from 831 to 841 nm, Am(VI) from 666 to 677 nm) (Figs. 2b-d), initially implying strong complexation between AnO_2^{2+} ions and the POM[15]. In particular, we performed a spectrophotometric titration of the ^{243}Am(VI)- {Se_6W_{46}} system to gain quantitative insight into the complexation process. The characteristic *f-f* transition band of free AmO_2^{2+} ions at 666 nm gradually decreases, while a new band at 677 nm emerges concurrently during the titration (Fig. 2d). Fitting these titration data suggests the formation of a 1:1 AmO_2^{2+}/{Se_6W_{46}} complex, and its formation constant (logβ)

was calculated as 6.0 (Fig. S4). This value confirms strong complexation between hexavalent actinyl ions and POM in 0.1 M nitric acid (Table S1). More importantly, the strong complexation stabilizes ^{243}Am(VI), and only 0.67% of the Am(VI) was reduced in the presence of POM clusters over a period of 24 hours (Fig. 2e) by radiolysis products. In addition, the reduction kinetics rate of Am(VI) in the POM system is only -6.21×10^{-4} mM/h, which is at least two orders of magnitude slower than that of the free AmO_2^{2+} ion by self-reduction and/or by organic species-induced reduction (Fig. 2f). The solution chemistry investigation demonstrates that Am(VI) could persist to a previously unachievable level for separation applications with the aid of strong complexation by inorganic POM clusters.

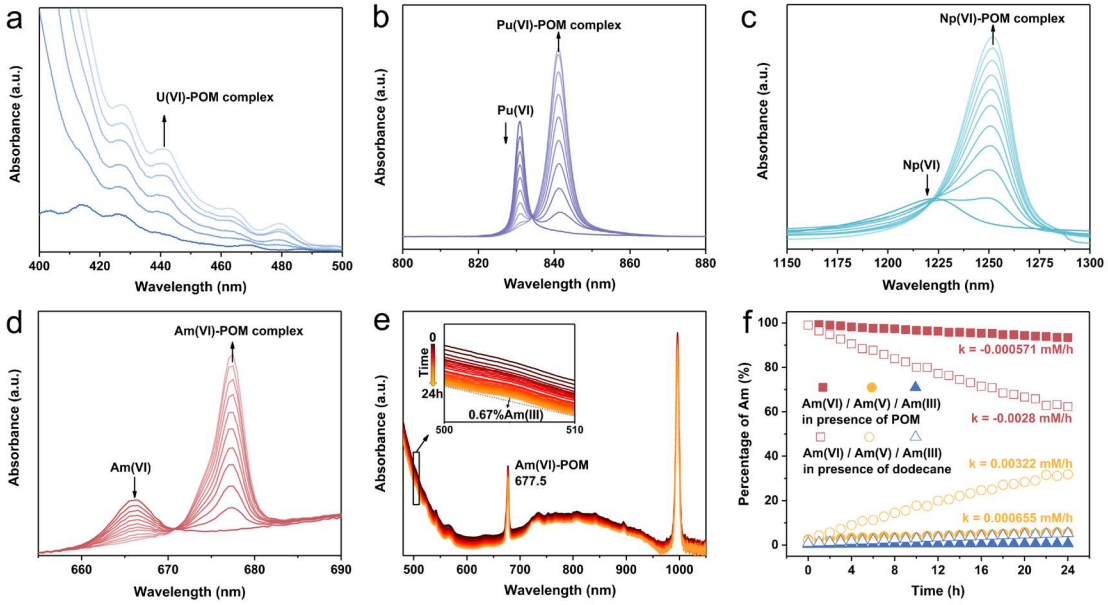

Fig. 2 Absorption spectra of An(VI)-POM in aqueous solution. a-d, Spectrophotometric titrations of POM complexing with hexavalent actinyl ions in 0.1 M HNO_3 aqueous solution, UO_2^{2+}, PuO_2^{2+}, NpO_2^{2+}, and AmO_2^{2+}. **e**, Change in the absorption spectra of the aqueous solution containing 0.25 mM Am in 0.1 M HNO_3, which was oxidized with copper(III) periodate, in the presence of 2.0 eq. POM over a period of 24 h. **f**, Autoreduction kinetics of Am(VI)-POM in 0.1 M HNO_3.

To directly visualize the interaction between AnO_2^{2+} ions and the POM cluster, we prepared a series of actinyl-POM crystals by reacting AnO_2^{2+} ions (An = ^{238}U, ^{237}Np, ^{242}Pu, or ^{243}Am) with $\{Se_6W_{46}\}$ in solution (Fig. 3a). Single crystal X-ray diffraction (SCXRD) analysis shows that actinyl-POMs from U to Am are isomorphous and crystallize in the monoclinic space group $P2_1/m$. The actinyl ions are fully encapsulated within the predesigned vacant site. The equatorial oxygen atoms of actinyl ions are provided by four distinct WO_6^{6-} groups and one coordinated water, forming a pentagonal bipyramid coordination geometry (Figs. 3b and 3c). To demonstrate the oxidation state of actinyl ions in the POM cluster, solid-state UV–vis-NIR absorption spectra were recorded on these single crystals. Fig. 3e shows the typical electronic transitions associated with *f*-elements in the hexavalent state, including charge-transfer

transitions at 349 nm (UO_2^{2+}) and Laporte-forbidden $5f \rightarrow 5f$ transitions at 841 nm (PuO_2^{2+}), 1242 nm (NpO_2^{2+}), 674 nm (AmO_2^{2+}). In addition, crystallographic investigation confirms that the actinide contraction effect dominates the An=O axial bond distances and An-O equatorial bond distances. In the actinyl-POM cluster, the average An=O axial bond distances are 1.741(2), 1.732(6), 1.703(4), and 1.700(3) Å for U^{VI}, Np^{VI}, Pu^{VI}, and Am^{VI}, respectively (Fig. 3d, Tables S2). Note that the An≡O axial bond distances in the POM are approximately 0.03 Å shorter than the bond distances in other oxoanion and organometallic compounds[16]. The different charge distributions in the interior and surface of POM tend to polarize the O≡An≡O axial bonds, thus leading to elongation of one bond and shortening of the other when the actinyl ion is vertically encapsulated within the vacancy site[17-19]. In sharp contrast, when Eu^{3+} ions, a representative Ln(III) ion, react with the POM under the same conditions, only pure $\{Se_6W_{46}\}$ crystals are isolated without the presence of any lanthanide ions in the structure.

A comparison of the binding energies for An(VI)-POM complexes (-508.26 to -491.22 kcal/mol) probed by DFT calculations shows that they are significantly larger than the values for complex formation of lanthanides with the POM cluster (-37.50 kcal/mol for Nd^{3+} and -37.74 kcal/mol for Eu^{3+}) because of pronounced electrostatic attraction and orbital interactions of actinyl ions with POM clusters when compared to lanthanides (Table S3 and Figs. S5-S7). Overall, the combination of crystallographic results, spectroscopy data, and computation results corroborate that the vacancy site in $\{Se_6W_{46}\}$ POM precisely matches the coordination geometry of actinyl(VI) ions and is unsuitable for binding Ln(III) ions.

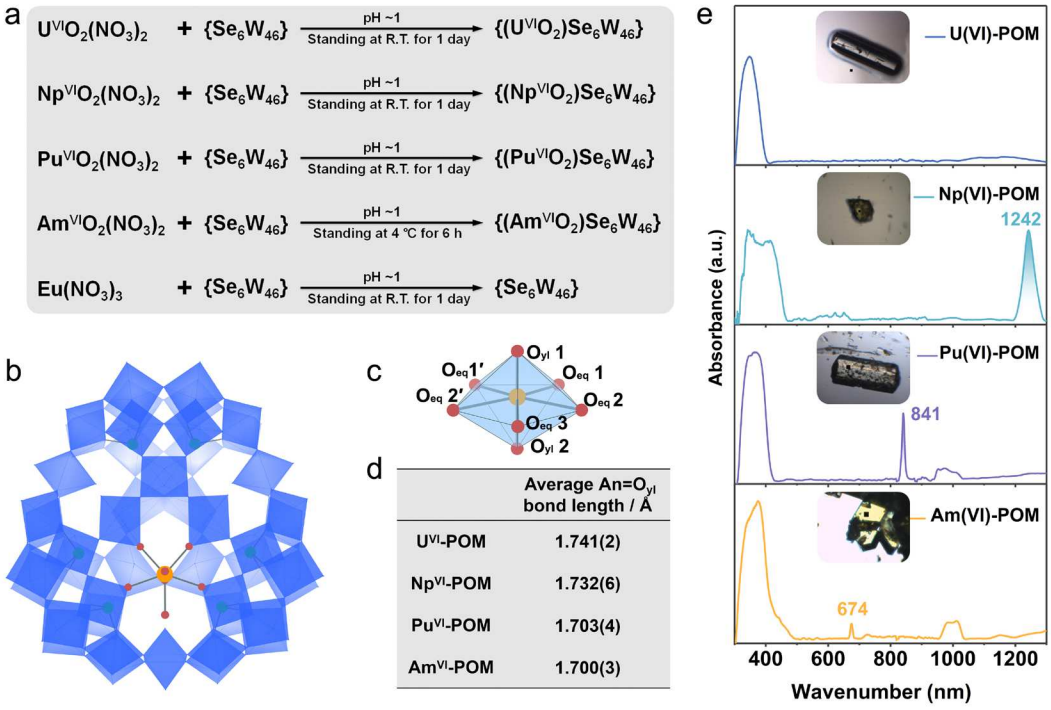

Fig. 3 Graphical representation of the structures of An-POM and absorption spectra of their single crystals. a, Chemical equations of POM assembled reactions with actinides or lanthanides. **b**, Polyhedral and ball and stick representation of Am(VI)-POM, with the H atoms and counterions omitted for clarity, Color code: blue octahedra, WO_6; orange ball, Am; red balls, O; green balls, Se. **c**, The pentagonal bipyramid coordination geometry of Am(VI). **d**, The table of average An≡O bond length. **e**, UV–Vis spectra of single crystal U(VI)-POM, Np(VI)-POM, Pu(VI)-POM, and Am(VI)-POM. Inset: the photograph of single crystals.

Owing to size and charge differences for Am(VI)-POM clusters and hydrated lanthanide ions in nitric acid solution, we designed a separation protocol relying on a commercially available ultrafiltration technique. The whole separation procedure using the oxidization of the actinides, nanoscale cluster assembly, and ultrafiltration separation, can be accomplished homogeneously within minutes using the aqueous solution with no organic component involved (Fig. 4a). This significantly reduces the amount of secondary radioactive waste. The purified Am(VI)-POM can be further reduced to obtain Am(III) products, while the released POM clusters can be recyclable again by ultrafiltration for the next separation cycle (Fig. 4a). After the screening of condition parameters such as acidity, reaction time, as well as the type and concentration of counterions (Figs. S8-10), we tested the optimized recovery of AnO_2^{2+} ions (An = ^{238}U, ^{237}Np, ^{242}Pu, or ^{243}Am) after the ultrafiltration process. As shown in Fig. 4b, the rejection coefficients and one-step recovery rates of actinyl ions are higher than 96% for U, Np, and Pu, and 92% for Am. The rejection coefficient of Eu^{3+} is low at 1.3%. These results give rise to a Am(VI)/Eu(III) separation factor of 873 that is significantly higher than those of all other americium oxidation associated separation techniques [20-27] (Fig. 4c).

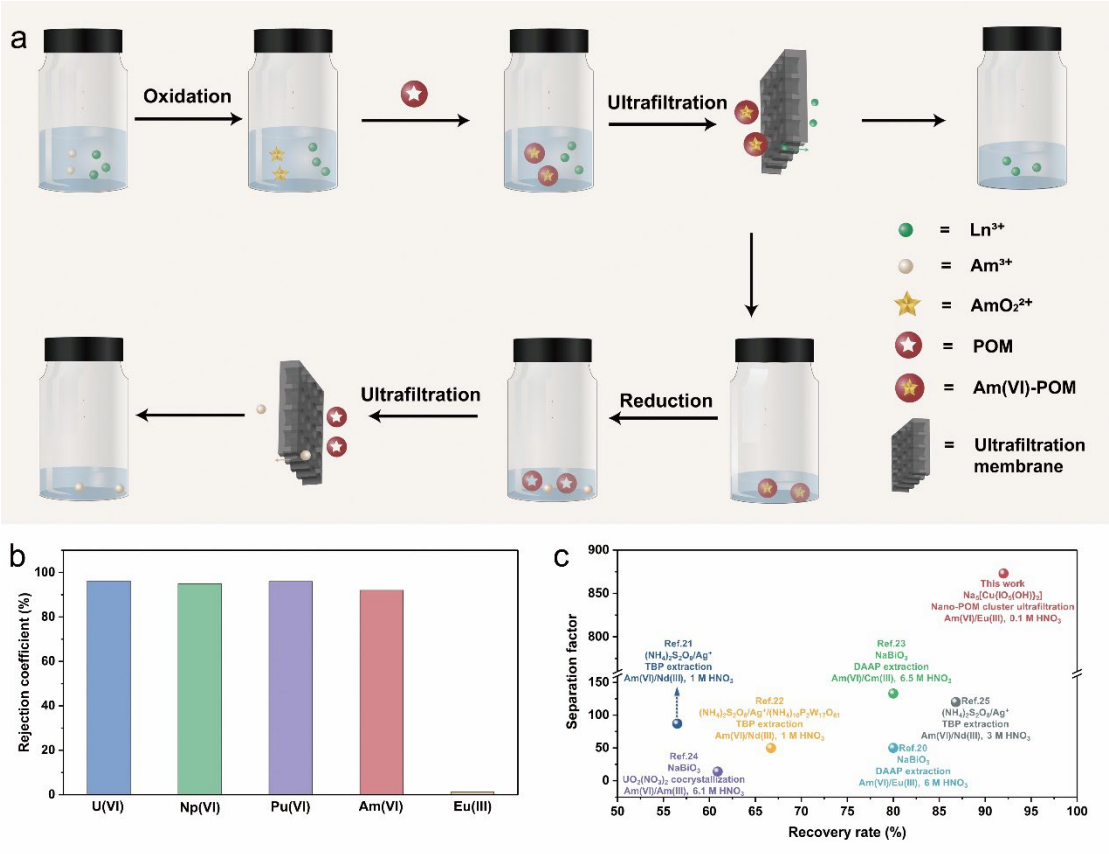

Fig. 4 Demonstration of Am separation through oxidation / complexing / ultrafiltration using POMs as complexants. a, Depiction of actinide group separation strategies. **b**, Ultrafiltration separation results of U(VI), Np(VI), Pu(VI), Am(VI), and Eu(III). The experimental condition: initial An(VI) or Eu(III) concentration is ~ 2.0×10^{-5} mol/L, POM concentration is ~ 4.0×10^{-5} mol/L, HNO_3 concentration is 0.1 mol/L, NH_4NO_3 concentration is 0.15 mol/L and reaction time is 5 minutes. **c**, Comparisons with the representative Am(VI) based separation performances on the recovery rate of Am and separation factor.

Conclusion

The foregoing results demonstrate that control of the lacunary structure in POM cluster enables the unprecedented complexation and stabilization of Am(VI) in aqueous solution, leading to a new separation strategy with merits of high efficiency, environmental friendliness, low time-cost, and low energy input. This idea also opens a new opportunity for actinide group separation from fission products during the used nuclear fuel reprocessing.

Reference

1. Kessler, G. Proliferation resistance of americium originating from spent irradiated reactor fuel of pressurized water reactors, fast reactors, and accelerator-driven systems with different fuel cycle options. *Nucl. Sci. Eng.* **159**, 56-82 (2008).
2. Magill, J. *et al*. Impact limits of partitioning and transmutation scenarios on the radiotoxicity of actinides in radioactive waste. *Nucl. Energy* **42**, 263-277 (2003).
3. Salvatores, M. Nuclear fuel cycle strategies including partitioning and transmutation. *Nucl. Eng. Des.* **235**, 805-816 (2005).
4. Peterman, D. R. *et al*. Selective extraction of minor actinides from acidic media using symmetric and asymmetric dithiophosphinic acids. *Sep. Sci. Technol.* **45**, 1711-1717 (2010).
5. Panak, P. J. & Geist, A. Complexation and extraction of trivalent actinides and lanthanides by triazinylpyridine N-donor ligands. *Chem. Rev.* **113,** 1199-1236 (2013).
6. Runde, W. H. & Mincher, B. J. Higher oxidation states of americium: preparation, characterization and use for separations. *Chem. Rev*. **111**, 5723-5741 (2011).
7. Mincher, B. J.,Martin, L. R. & Schmitt, N. C. Diamylamylphosphonate solvent extraction of Am (VI) from nuclear fuel raffinate simulant solution. *Solv. Extract. Ion Exch*. **30**, 445-456 (2012).
8. Moyer, B. A., Lumetta, G. J. & Mincher, B. J. Minor actinide separation in the reprocessing of spent nuclear fuels: Recent advances in the United States. *Reprocessing and Recycling of Spent Nuclear Fuel* chapter **11**, 289-312 (2015).
9. Stephanou, S. E. & Penneman, R. A. Observations on curium valence states; A rapid separation of americium and curium. *J. Am. Chem. Soc.* **74,** 3701-3702 (1952).
10. Hulet, E. K. An investigation of the extraction-chromatography of Am (VI) and Bk (IV). *J. Inorg. Nucl. Chem.* **26,** 1721-1727 (1964).
11. Dares, C. J., Lapides, A. M., Mincher, B. J. & Meyer, T. J. Electrochemical oxidation of ^{243}Am(III) in nitric acid by a terpyridyl-derivatized electrode. *Science* **350**, 652-655 (2015).
12. Gouzerh, P. & Proust, A. Main-group element, organic, and organometallic derivatives of polyoxometalates. *Chem. Rev.* **98**, 77-112 (1998).
13. Kalinina, I. V. *et al*. Cyclic tungstoselenites based on $\{Se_2W_{12}\}$ units. *Inorg. Chem.* **53**, 2076-2082 (2014).
14. Cameron, J. M., Gao, J., Vilà-Nadal, L.,Long, D.-L. & Cronin, L. Formation, self-assembly and transformation of a transient selenotungstate building block into clusters, chains and macrocycles. *Chem. Commun.* **50**, 2155-2157 (2014).

15. Xu, C., Tian, G., Teat, S. J. & Rao, L. Complexation of U (VI) with dipicolinic acid: thermodynamics and coordination modes. *Inorg. Chem.* **52**, 2750-2756 (2013).

16. Krivovichev, S. V. & Burns, P. C. Actinide compounds containing hexavalent cations of the VI group elements (S, Se, Mo, Cr, W). *Structural Chemistry of Inorganic Actinide Compounds* chapter **4**, 95-182 (2007).

17. Kim, K.-C. & Pope, M. T. Cation-directed structure changes in polyoxometalate chemistry. Equilibria between isomers of bis (9-tungstophosphatodioxouranate (VI)) complexes. *J. Am. Chem. Soc.* **121**, 8512-8517 (1999).

18. Talbot-Eeckelaers, C. *et al*. Luminescence from neptunyl (VI) species in solution. *J. Am. Chem. Soc.* **129**, 2442-2443 (2007).

19. Copping, R. *et al*. Probing the 5f electrons in a plutonyl (VI) cluster complex. *Dalton Trans.* **29**, 5609-5611 (2009).

20. Mincher, B. J., Martin, L. R. & Schmitt, N. C. Diamylamylphosphonate solvent extraction of Am (VI) from nuclear fuel raffinate simulant solution. *Solv. Extract. Ion Exch*. 30, 445-456 (2012).

21. Kamoshida, M. & Fukasawa, T. Solvent extraction of americium(VI) by tri-n-butyl phosphate. *J. Nucl. Sci. Technol.* **33**, 403-408 (1996).

22. Kamoshida, M., Fukasawa, T. & Kawamura, F. Valence control and solvent extraction of americium in the presence of ammonium phosphotungstate. *J. Nucl. Sci. Technol.* **35**, 185-189 (1998).

23. Mincher, B. J. *et al*. Characterizing diamylamylphosphonate (DAAP) as an americium ligand for nuclear fuel-cycle applications. *Solv. Extract. Ion Exch*. **32**, 153-166 (2014).

24. Burns, J. D. & Moyer, B. A. Group hexavalent actinide separations: a new approach to used nuclear fuel recycling. *Inorg. Chem.* **55**, 8913-8919 (2016).

25. Koma, Y., Aoshima, A., Kamoshida, M. & Sasahira, A. Extraction of Am (VI) from nitric acid solution containing phosphate anion by TBP. *J. Nucl. Sci. Technol.* **3**, 317-320 (2002).

26. McCann, K., Brigham, D. M., Morrison, S. & Braley, J. C. Hexavalent americium recovery using copper (III) periodate. *Inorg. Chem.* **55**, 11971-11978 (2016).

27. McCann, K., Mincher, B. J., Schmitt, N. C. & Braley, J. C. Hexavalent actinide extraction using N,N-Dialkyl amides. *Ind. Eng. Chem. Res.* **56**, 6515-6519 (2017).

Methods

General considerations

Cations! The isotopes of Np, Pu, and Am exhibit significant radio- and chemo-toxicity and represent serious health risks when inhaled or digested. ^{237}***Np (***$t_{1/2}$ ***= 2.14 × 10^6 *** ***years, 0.7 mCi/g) is a strong α emitter, and decays to the short-lived isotope*** ^{233}***Pa (***$t_{1/2}$ ***= 27.0 days), which is a potent β and γ emitter.*** ^{242}***Pu (***$t_{1/2}$ ***= 3.76 × 10^5 *** ***years, specific activity = 3.9 mCi/g) is a strong α emitter.*** ^{243}***Am (***$t_{1/2}$ ***= 7,380 years; specific activity = 199 mCi/g) is a strong α emitter with γ emission, presenting internal and external radiotoxic hazards. All experimental studies were conducted in a licensed laboratory dedicated to transuranium elements study with approved safety operating procedures. All neptunium, plutonium, and americium materials have to be handled either in negative-pressure radiological fume hoods or glove boxes equipped with high efficiency particulate air (HEPA) filters while high-level precautions and procedures for handling radioactive materials must be followed.***

All reagents were purchased from chemical reagent suppliers and used without further purification. Millipore water was used in all experiments. The POM precursor of $\{Se_6W_{39}\}$ was synthesized according to the previously reported procedure[13]. $^{237}NpO_2$ powder was obtained from the China Institute of Atomic Energy (CIAE). $^{242}PuO_2$ powder and $^{243}AmO_2$ powder were purchased from the Shenzhen Isotope Industrial International Co., Ltd., which are originally produced in Los Alamos National Laboratory, U.S. (sample identification of No. Pu-242-237-A and Am-1-91-Prod). In the $^{242}PuO_2$ sample, the weight ratio of ^{242}Pu, ^{238}Pu, ^{239}Pu, ^{240}Pu, ^{241}Pu, ^{244}Pu are 99.9628 %, 0.0029 %, 0.0049 %, 0.0217 %, 0.0056 %, and 0.0020 %, respectively. In the $^{243}AmO_2$ sample, the weight ratio of ^{243}Am, ^{241}Am, ^{242}Am are 99.987 %, 0.012 %, and < 0.001 %, respectively. The oxidation of Am(III) to Am(VI) in aqueous solution was achieved by Cu(III) periodate oxidant according to the reported procedure[28].

Synthesis

$[(CH_3)_2NH_2]_{16}H_{16}[Se_6W_{46}O_{166}(H_2O)_3]\cdot 15H_2O$ ($\{Se_6W_{46}\}$)

150 mg $\{Se_6W_{39}\}$ was dissolved in 2 mL water, and then 2 mL $(CH_3)_2NH_2Cl$ aqueous solution (75 mg/mL), 1 mL water, and 0.2 mL HNO_3 (8 mol/L) were added. Colorless crystals were obtained after 24 hours. Yield: 0.074 g. (46% based on W). Calcd for $Se_6W_{46}C_{32}N_{16}O_{184}H_{384}$: Se, 3.74; C, 3.03; N, 1.76; H 1.43. Found: Se, 3.72; C, 3.18; N, 1.68; H, 1.34.

$[(CH_3)_2NH_2]_{14}H_{16}[(U^{VI}O_2)Se_6W_{46}O_{166}(H_2O)_4]\cdot xH_2O$ (U(VI)-POM)

170 mg of $\{Se_6W_{46}\}$ was dissolved in 2 mL HNO_3 solution (0.1 mol/L), and then 2.0 mL of HNO_3 solution (0.1 mol/L) containing 150 mg $(CH_3)_2NH_2Cl$ was added. After that, 1.0 mL of HNO_3 solution (0.1 mol/L) containing $UO_2(NO_3)_2\cdot 6H_2O$ (5.5 mg, 0.011 mmol) was added slowly to the prepared POM solution with stirring. Yellow rod-shaped crystals of U(VI)-POM were isolated at room temperature after 1 day.

$[(CH_3)_2NH_2]_{14}H_{16}[(Np^{VI}O_2)Se_6W_{46}O_{166}(H_2O)_4]\cdot xH_2O$ (Np(VI)-POM)

35 mg of $\{Se_6W_{46}\}$ was dissolved in 400 μL HNO_3 solution (0.1 mol/L), and then 400 μL of HNO_3 solution (0.1 mol/L) containing 30 mg $(CH_3)_2NH_2Cl$ was added. After that, a stock solution of $Np^{VI}O_2^{2+}$ nitrate containing 1.0 mg Np(VI) was slowly added into the prepared POM solution. Light yellow rod-shaped crystals of Np(VI)-POM were isolated at room temperature after 1 day.

$[(CH_3)_2NH_2]_{14}H_{16}[(Pu^{VI}O_2)Se_6W_{46}O_{166}(H_2O)_4]\cdot xH_2O$ (Pu(VI)-POM)

35 mg of $\{Se_6W_{46}\}$ was dissolved in 400 μL HNO_3 solution (0.1 mol/L), and then 400 μL of HNO_3 solution (0.1 mol/L) containing 30 mg $(CH_3)_2NH_2Cl$ was added. After that, a stock solution of

$Pu^{VI}O_2^{2+}$ nitrate containing 1.0 mg Pu(VI) was slowly loaded into the prepared POM solution. Light yellow rod-shaped crystals of Pu(VI)-POM were isolated at room temperature after 1 day.

$K_{14}H_{16}[(Am^{VI}O_2)Se_6W_{46}O_{166}(H_2O)_4]\cdot xH_2O$ (Am(VI)-POM)

Addition of 2.5 mg Cu(III) periodate into the 100 μL Am^{3+} solution (0.6 mg Am^{3+} in mass) generated the $Am^{VI}O_2^{2+}$ solution. Then, 3.5 mg of $\{Se_6W_{46}\}$ dissolved in 40 μL HNO_3 solution (0.1 mol/L) was added. After that, 3.0 mg KNO_3 dissolved in 40 μL HNO_3 solution (0.1 mol/L) was added to the solution. The mixed solution was stored in a freezer (4 °C) for reaction. Golden yellow block crystals were isolated after 6 hours.

UV-Vis-NIR Spectrophotometric Titration

The UV-vis-NIR spectra were collected with a Cary 5000 spectrophotometer (Agilent, USA) using quartz cuvettes with a 1 cm pathlength, with the configuration of bandwidth of 0.5 nm and an integration time of 0.10 seconds. Typically, 0.400 mL of Am(VI) (~ 0.2 mM) in a 1.0 cm quartz cell was titrated with the POM solution (0.8 mM, 10 μL per addition) through a 10 μL pipette. After each addition, the solutions were electromagnetically stirred for 5 minutes before recording the spectra. Preliminary kinetic experiments demonstrated that the reaction reaches equilibrium under 5 minutes. The formation constants were then calculated by nonlinear regression using the program of HypSpec[29] based on the obtained spectral data. The titration procedures for Pu(VI), Np(VI), and U(VI) were similar to that for Am(VI).

Solid-state UV-vis-NIR spectroscopy

Solid-state UV-vis-NIR spectra were recorded using a Craic Technologies microspectrophotometer. Crystals (except for Am(VI)-POM) were placed on a quartz slide under immersion oil and the data were collected from 400 to 1300 nm under room temperature. Because the americium(VI) in the crystal of Am(VI)-POM will be reduced by the oil, it is necessary to avoid immersing the crystal in the oil.

Crystallographic studies

Single crystal X-ray diffraction data were mounted on a loop for the X-ray measurement. Diffraction data were collected on Bruker D8-Venture diffractometer with a Turbo X-ray Source (Mo-Kα radiation, λ = 0.71073 Å) adopting the direct-drive rotating anode technique and a CMOS detector at room temperature. The data frames were collected using the program APEX3 and processed using the program SAINT routine in APEX3. Using Olex2[30], the structure was solved by the ShelXT[31] structure solution program using Intrinsic Phasing and refined with the ShelXL[32] refinement package using Least Squares minimization. The solvate molecules and counterions of all data were treated as a diffuse contribution to the overall scattering without specific atom positions by SQUEEZE/PLATON[33] due to their severe disorder in the lattices.

Computational details

All the theoretical calculations were carried out at the level of density functional theory (DFT) using the Amsterdam Density Functional program (ADF 2019.301)[34]. The theoretical results were performed within the generalized gradient approximation (GGA) with the PBE exchange-correlation functional[35]. The zero-order-regular approximation (ZORA)[36] was adopted to account for the scalar relativistic effects. And the TZ2P, TZP (containing valence triple zeta and two or one polarization function), and DZP (containing valence double zeta and one polarization function) basis sets were employed as TZ2P for U, Np, Pu, Am, Nd, Eu, and TZP for W and DZP for H, O and Se[37]. The frozen core approximation was used as [$1s^2$-$4f^{14}$] for U, Np, Pu, Am, W, [$1s^2$-$4d^{10}$] for Nd, Eu, [$1s^2$-$3d^{10}$] for Se and [$1s^2$] for O. The conductor-like screening model (COSMO)[38] was also used

with the water environment. Besides, the energy decomposition analysis with natural orbitals for chemical valence (EDA-NOCV)[39, 40] was calculated to analyze the chemical bonding properties using the ADF 2019.301 program.

Separation method and separation factor determination.

The ultrafiltration separation of $U^{VI}O_2^{2+}/Eu^{3+}$ was conducted at room temperature. The pH was adjusted by adding a small volume of concentrated HNO_3. The solution of POM was added in the solution of $U^{VI}O_2^{2+}/Eu^{3+}$, then the solution of NH_4NO_3 was added. The mixed solution was shaken several times on a shaker at room temperature and transferred to a centrifugal concentrator (Pall, modified polyethersulfone ultrafiltration membrane with 3kDa MWCO). They were centrifuged to separate the An-POM complexes from lanthanide ions. The concentrations of U and Eu in the initial solution and final filtrate were determined by ICP-AES and ICP-MS, respectively. The rejection coefficient (*R*) and the separation factor (*SF*) were calculated from the following equation:

$$R = (1 - \frac{c_p}{c_f}) * 100\% \quad (1)$$

$$SF_{U/Eu} = (\frac{c_f - c_p}{c_p})_U / (\frac{c_f - c_p}{c_p})_{Eu} \quad (2)$$

where c_f and c_p are the concentration of metal ion in the feed and permeate streams, respectively.

The ultrafiltration separations of Pu(VI), Np(VI), and Am(VI) by POM $\{Se_6W_{46}\}$ were conducted at room temperature. The solution of POM in 0.1 M HNO_3 solution was added in the solution of Pu(VI), Np(VI), and Am(VI). Then, the solution of NH_4NO_3 was added. The mixed solution was shaken several times on a shaker at room temperature and transferred to a centrifugal concentrator (Pall, modified polyethersulfone ultrafiltration membrane with 3kDa MWCO). The systems were centrifuged to retain the An-POM complexes. The amount of An(VI) was determined by taking an aliquot of 0.100 mL sample of the initial solution and the filtrate and mixing it with 10 mL of a scintillation cocktail for liquid scintillation counting on an ultra-low background liquid-scintillation spectrometer (Quantulus 1220, Perkin Elmer, USA). The rejection coefficient (*R*) for a given radioisotope was calculated from the following equation:

$$R = (1 - \frac{C_p}{C_f}) * 100\% \quad (3)$$

where C_f and C_p are the counting rates (CPM) of the radioactive nuclides per unit volume in the feed and permeate streams, respectively.

To quantify the separation between An(VI) and Eu(III), the theoretical separation factor (*SF*) was calculated by the formula:

$$SF_{An/Eu} = (\frac{R}{1-R})_{An} / (\frac{R}{1-R})_{Eu} \quad (4)$$

where *R* is the rejection coefficient.

Data availability

The crystallographic data have been deposited at the Cambridge Crystallographic Data Center with reference number CCDC 2150690-2150694. This data can be obtained free of charge from The Cambridge Crystallographic Data Centre via http://www.ccdc.cam.ac.uk/data_request/cif.

Methods references

28. Sinkov, S. I. & Lumetta, G. J. Americium (III) oxidation by copper (III) periodate in nitric acid solution as compared with the action of Bi (V) compounds of sodium, lithium, and potassium. *Radiochim. Acta* **103**, 541-552 (2015).

29. Gans, P., Sabatini, A. & Vacca, A. Investigation of equilibria in solution. Determination of equilibrium constants with the HYPERQUAD suite of programs. *Talanta* 43, 1739-1753 (1996).

30. Dolomanov, O. V. *et al.* OLEX2: a complete structure solution, refinement and analysis program. *J. Appl. Crystallogr. **42**, 339-341* (2009).

31. Sheldrick, G. M. SHELXT – integrated space-group and crystal-structure determination. *Acta Crystallogr. A* **71**, 3–8 (2015).

32. Sheldrick, G. M. Crystal structure refinement with SHELXL. *Acta Crystallogr.* C**71**, 3-8 (2015).

33. Spek, A. L. PLATON SQUEEZE: a tool for the calculation of the disordered solvent contribution to the calculated structure factors. *Acta Crystallogr.* C **71**, 9–18 (2015).

34. Velde, G. *et al.* Chemistry with ADF. *J. Comput. Chem.* **22**, 931-967 (2001).

35. Perdew, J. P., Burke, K. & Ernzerhof, M. Generalized gradient approximation made simple. *Phys. Rev. Lett*. **77**, 3865-3868 (1996).

36. Lenthe, E., Baerends, E. J. & Snijders, J. G. Relativistic regular two-component Hamiltonians. *J. Chem. Phys*. **99**, 4597-4610 (1993).

37. Lenthe, E. & Baerends, E. J. Optimized Slater-type basis sets for the elements 1–118. *J. Comput. Chem.* **24**, 1142-1156 (2003).

38. Klamt, A. & Schüürmann, G. COSMO: a new approach to dielectric screening in solvents with explicit expressions for the screening energy and its gradient. *J. Chem. Soc., Perkin Trans. 2* **5**, 799-805 (1993).

39. Michalak, A. Mitoraj, M. & Ziegler, T. Bond orbitals from chemical valence theory. *J. Phys. Chem. A* **112**, 1933–1939 (2008).

40. Mitoraj, M. P., Michalak, A. & Ziegler, T. A combined charge and energy decomposition scheme for bond analysis. *J. Chem. Theory Comput.* **5**, 962–975 (2009).

Acknowledgements

We are grateful funding support from the National Natural Science Foundation of China (21790374, 21825601, 21806118, 22006106), and the Natural Science Foundation of Jiangsu Province (BK20211546). T. E. A.-S. was supported by the U.S. Department of Energy, Office of Basic Energy Sciences, Solar Photochemistry program under award number DE-SC0021372.

Author contributions

S. W., T. E. A.-S., and Y. W. conceived and supervised the project. H. Z., Y. W., A. L., K. L. designed the materials and performed the oxidation experiment, separation experiment, crystal growth, and structural determination. M. V. S. performed the oxidation experiment as well. E. V. A. assisted with resolving crystal structures. H. Z., Z. W. and C. X. performed solution chemistry investigations. X. X. and H.-S. H. performed the calculations. Z. C. aided to the discussion. S. W., TEA-S, Y. W., H.

Z., and C. X. prepared the manuscript. All authors discussed the results and commented on the manuscript.

Competing interests

T. W., Y. W. and H. Z. and Soochow University have filed a patent on the presenting results. All other authors declare no competing financial interests.

Additional information

Supplementary information The online version contains supplementary material available at XX.

Correspondence and requests for materials should be addressed to Y. W., C. X., T. E. A.-S. or S.W.

Peer review information *Nature* thanks the anonymous reviewers for their contribution to the peer review of this work. Peer reviewer reports are available.

Reprints and permissions information is available at http://www.nature.com/reprints.

Supplementary Files

This is a list of supplementary files associated with this preprint. Click to download.

- SIAmPOMSchoenzart2022.pdf